

A Study of Light Mesons on the Transverse Lattice

Matthias Burkardt and Sudip K. Seal

Department of Physics

New Mexico State University

Las Cruces, NM 88003-0001

U.S.A.

Abstract

We present results from a study of light meson spectra and structure obtained within the framework of light-front QCD formulated on a transverse lattice. We discuss how imposing Lorentz covariance conditions on meson dispersion relations allows determination of parameters in the transverse lattice Hamiltonian. The pion distribution amplitude obtained in this framework is rather close to its asymptotic shape.

I. INTRODUCTION

Many high energy scattering experiments probe hadron structure very close to the light-cone. Hence correlation functions probed in such experiments have a particularly simple physical interpretation in the light-front (LF) framework (or infinite momentum frame), i.e. in a Hamiltonian framework where $x^+ \equiv x^0 + x^3$ is ‘time’. For example, parton distribution functions measured in deep-inelastic scattering experiments provide information about the LF momentum distribution of quarks in the target hadron. Off-forward parton distributions, probed in deeply virtual Compton scattering, have the interpretation of matrix elements of the LF momentum density operator between states of unequal momenta. Furthermore, the pion distribution amplitude, relevant for example for the asymptotic pion form factor, can

be related to the LF wavefunction for the pion in the $q\bar{q}$ Fock component when q and \bar{q} have the same \perp position.

Even though these important observables have their most physical interpretation on the LF, it is, at least in principle, possible to calculate them in any approach to QCD. However, what distinguishes the LF framework from all other formulation of QCD is that the above observables have a very direct and physical connection to the microscopic degrees of freedom in terms of which the Hamiltonian is constructed. Because of this unique feature, it should be much easier in this framework to gain a physical understanding between experiment and phenomenology on the one hand and the underlying QCD dynamics on the other.

Other motivations to study QCD formulated on the LF derive from the fact that the complexity of the vacuum seemingly shifts from the states to the operators in this framework [1]. This results in a separation between the physics of the vacuum and the parton structure of hadrons which implies for example that a constituent picture of hadrons has a chance to make sense [2].

Of course, just like in any other approach to QCD, it is necessary to regularize both UV and IR divergences before one can even attempt to perform nonperturbative calculations. The transverse lattice [3] is an attempt to combine advantages of the LF and lattice formulations of QCD. In this approach to LF-QCD the time and one space direction (say x^3) are kept continuous, while the two ‘transverse’ directions $\mathbf{x}_\perp \equiv (x^1, x^2)$ are discretized. Keeping the time and x^3 directions continuous has the advantage of preserving manifest boost invariance for boosts in the x^3 direction. Furthermore, since $x^\pm = x^0 \pm x^3$ also remain continuous, this formulation still allows a canonical LF Hamiltonian approach. On the other hand, working on a position space lattice in the transverse direction allows one to introduce a gauge invariant cutoff on \perp momenta — in a manner that is similar to Euclidean or Hamiltonian lattice gauge theory.

In summary, the LF formulation has the advantage of utilizing degrees of freedom that are very physical since many high-energy scattering observables (such as deep-inelastic scattering cross sections) have very simple and intuitive interpretations as equal LF-time (x^+)

correlation functions. Using a gauge invariant (position space-) lattice cutoff in the \perp direction within the LF framework has the advantage of being able to avoid the notorious $1/k^+$ divergences from the gauge field in LF-gauge which plague many other Hamiltonian LF approaches to QCD [4].

The hybrid treatment (continuous versus discrete) of the longitudinal/transverse directions implies an analogous hybrid treatment of the longitudinal versus transverse gauge field: the longitudinal gauge field degrees of freedom are the non-compact A^μ while the transverse gauge degrees of freedom are compact link-fields. Each of these degrees of freedom depend on two continuous (x^\pm) and two discrete (\mathbf{n}_\perp) space-time variables, i.e. from a formal point of view the canonical transverse lattice formulation is equivalent to a large number of coupled $1 + 1$ dimensional gauge theories (the longitudinal gauge fields at each \mathbf{n}_\perp) coupled to nonlinear σ model degrees of freedom (the link fields) [5].

For a variety of reasons it is advantageous to work with transverse gauge degrees of freedom that are general matrix fields rather than $U \in SU(N_C)$. First of all, we would like to work at a cutoff scale which is small (in momentum scale) since only then do we have a chance to find low lying hadrons that are simple (i.e. contain only few constituents). If one wants to work on a very coarse lattice, it is useful to introduce smeared or averaged degrees of freedom. Upon averaging over neighboring ‘chains’ of $SU(N_C)$ fields one obtains degrees of freedom which still transform in the same way as the original $SU(N_C)$ degrees of freedom under gauge transformations but are general matrix degrees of freedom no longer obeying $U^\dagger U = 1$ and $\det(U) = 1$. The price that one has to pay for introducing these smeared degrees of freedom are more complicated interactions. The advantage is that low lying hadrons can be described in a Fock expansion (this has been confirmed by calculations of the static quark-antiquark potential [6] and glueball spectra [7]).

Another important advantage of this ‘color-dielectric’ approach is that it is much easier to construct a Fock expansion of states out of general linear matrix fields than out of fields that are subject to non-linear $SU(N_C)$ constraints.

In the color-dielectric approach the complexity is shifted from the states to the Hamil-

tonian: In principle, there exists an exact prescription for the transformation from one set of degrees of freedom (here U 's) to blocked degrees of freedom $M \equiv \sum_{av} \prod_i U_i$

$$e^{-S_{eff.}(M)} = \int [dU] e^{-S_{can.}(U)} \delta \left(M - \sum_{av} \prod_i U_i \right). \quad (1.1)$$

The problem with this prescription is that $S_{eff.}$ is not only very difficult to determine directly, but in general also contains arbitrarily complicated interactions.

A much more practical approach towards determining the effective interaction among the link fields nonperturbatively is the use of Lorentz invariance. This strategy has been used in a systematic study of glueball masses in Ref. [7], where more details can be found regarding the effective interaction. One starts by making the most general ansatz for the effective interaction which is invariant under those symmetries of QCD that are not broken by the \perp lattice. This still leaves an infinite number of possible terms and for practical reasons, only terms up to fourth order in the fields and only local (in the \perp direction) terms have been included in the Ref. [7]. The coefficients of the remaining terms are then fitted to maximize Lorentz covariance for physical observables, such as the $Q\bar{Q}$ potential (rotational invariance!) and covariance of the glueball dispersion relation. It should be emphasized that these are first principle calculations in the sense that the only phenomenological input parameter is the overall mass scale (which can for example be taken to be the lowest glueball mass or the string tension). The only other input that is used is the requirement of Lorentz invariance.

The numerical results from Refs. [7,6] within this approach are very encouraging:

- with only a few parameters, approximate Lorentz invariance could be achieved for a relatively large number of glueball dispersion relations simultaneously [7] as well as for the $Q\bar{Q}$ potential
- the glueball spectrum that was obtained numerically on the \perp lattice for $N_C \rightarrow \infty$ is consistent with Euclidean Monte Carlo lattice gauge theory calculations performed at finite N_C and extrapolated to $N_C \rightarrow \infty$.

For further details on these very interesting results, the reader is referred to Refs. [7,6] and references therein. In this paper, we are applying this program to mesons on the transverse lattice within the femtoworm approximation [8]. This Hamiltonian has already been analyzed in Ref. [8] for mesons with $\vec{k}_\perp = 0$. In this work, as well as in a related independent paper [9], the work from Ref. [8] is generalized to mesons with nonzero transverse momenta. This generalization allows one to address the issue of Lorentz invariance of meson spectra. There are significant differences in the general approach between our work and Ref. [9]. First of all, while we employ continuous basis function techniques to solve the longitudinal dynamics, Refs. [9,11] use discrete light-cone quantization (DLCQ). Secondly, there is also a difference in the procedure: both this work and Ref. [11] use a longitudinal gauge coupling taken from pure glue calculations, while Ref. [9] refits this parameter. The latter difference has important consequences which we discuss in detail in section III. Our results confirm some of the results presented in Ref. [11], which serves as a non-trivial test for both approaches. However, the main motivation for our work lies in a different direction. Our goal was to understand to what extent the requirement of imposing Lorentz invariance sufficiently constrains the parameters of the Hamiltonian first studied in Ref. [8] and also to investigate whether this Hamiltonian and the femtoworm approximation are able to yield Lorentz invariant results. The paper is organized as follows. We briefly describe the Hamiltonian, the approximations used to solve it and some of its subtle properties in section II. In section III, we provide a perturbative analysis of the $\pi - \rho$ splitting. The results from this section will be of importance for understanding the non-perturbative numerical results presented in section IV. This is followed by some comments and comparisons of this work with another concurrent work in section V and a brief summary in section VI.

II. THE HAMILTONIAN

The transverse lattice Hamiltonian for Wilson fermions that forms the basis of our work and Ref. [11] was first constructed in Ref. [8], and we refer the reader to these works for

more details. Here we restrict ourselves to a more qualitative description of the degrees of freedom that enter the Hamiltonian and we follow up later with more specifics when we discuss the integral equations describing mesons in the femtoworm approximation. The degrees of freedom that enter the Hamiltonian are quark and antiquark creation operators at each site and link-fields (which, in the spirit of the color-dielectric approach [7], we take as general matrix fields) on the transverse links connecting the sites. For simplicity, we work in the large N_C limit. The first approximation that we use is a light front Tamm-Dancoff truncation of the Fock state expansion upto and including the 3-particle sector. Upon reminding oneself that the fermion degrees of freedom (quarks and antiquarks) always occupy the lattice (transverse) sites and the gauge degrees of freedom (link fields) reside on the lattice spacings, it is easy to understand the following two direct consequences of the aforementioned truncation:

- The 2-particle states consist of a quark and an antiquark sitting on the same lattice site.
- The 3-particle states consist of a quark and an antiquark separated by **at most** one link field.

Since link fields always reside on the lattice spacings as demanded by gauge invariance, the 3-particle Fock space is therefore spanned by all different configurations of a quark and an antiquark separated by one link field. This dumb-bell shaped configuration of the 3-sector naturally requires one to introduce an index to specify it's transverse orientation. We do so as shown in Fig. 1.

In keeping with the truncated Fock space, one can therefore write the meson state vector as:

$$|meson\rangle = c_2 |q\bar{q}\rangle + c_3 |q\bar{q}g\rangle \quad (2.1)$$

The total angular momentum of the fermions in the 2-sector is contributed wholly by their respective spins since there is no contribution from orbital angular momentum when they

are both on the same site. On the other hand, the total angular momentum of the 3-particle configuration is the sum of both their spins as well as the orbital angular momentum typical of dumb-bell shaped systems. To characterize a 2-particle state, one needs the spins of the two quarks along with their momenta, both longitudinal as well as transverse. Additionally, a 3-particle state will require the direction of it's configuration (see Fig. 1) in the discretized xy directions. The Hamiltonian, however, remains invariant when translated in multiples of the transverse lattice spacing. Consequently, the transverse momenta of the mesons are conserved (modulo π). This allows one to solve the light front Hamiltonian equation, $H_{LF} | \psi \rangle = P^- | \psi \rangle$, for fixed values of the transverse momentum, k_\perp . For a given value of k_\perp we therefore make the following ansatz:

$$| q\bar{q} \rangle = \sum_{\vec{n}_\perp} e^{i\vec{k}_\perp \cdot \vec{n}_\perp} \int_0^1 dx b_{s_1}^\dagger(x, \vec{n}_\perp) d_{s_2}^\dagger(1-x, \vec{n}_\perp) \psi_{s_1, s_2}(x) | 0 \rangle \quad (2.2)$$

$$| q\bar{q}g \rangle = \sum_{\vec{n}_\perp} e^{i\vec{k}_\perp \cdot (\vec{n}_\perp + \frac{\vec{e}_i}{2})} \int_0^1 dx \int_0^{1-x} dy b_{s_1}^\dagger(x, \vec{n}_\perp) d_{s_2}^\dagger(y, \vec{n}_\perp + \vec{e}_i) a^\dagger(1-x-y) \psi_{s_1, s_2}(x, y, \vec{e}_i) | 0 \rangle \quad (2.3)$$

where the spin degrees of freedom, $s_1, s_2 \in (\uparrow, \downarrow)$ and the orbital degrees of freedom, $\vec{e}_i \in (\pm\vec{e}_x, \pm\vec{e}_y)$. In the above, $\psi_{s_1, s_2}(x)$ and $\psi_{s_1, s_2}(x, y, \vec{e}_i)$ are the wavefunction amplitudes in the 2-particle and 3-particle sectors respectively. It is a straight forward though tedious procedure to show that the QCD Hamiltonian with the above state vectors in the large N_c limit and under the light front gauge yields the following integral equations in terms of the wavefunction amplitudes in the 2-particle and 3-particle sectors respectively:

$$H_{22}\psi_{s_1, s_2}(x) = \left(\frac{m_q^2 - 1}{x} + \frac{m_{\bar{q}}^2 - 1}{1-x} \right) \psi_{s_1, s_2}(x) - \int_0^1 dx' \frac{\psi_{s_1, s_2}(x')}{(x-x')^2} \quad (2.4)$$

$$H_{33}\psi_{s_1, s_2}(x, y, \vec{e}_i) = \left(\frac{m_q^2 - 1}{x} + \frac{m_{\bar{q}}^2 - 1}{y} + \frac{m_U^2}{1-x-y} \right)$$

$$\begin{aligned}
& \psi_{s_1, s_2}(x, y, \vec{e}_i) - \int_0^{1-y} dx' \frac{\psi_{s_1, s_2}(x', y, \vec{e}_i)}{(x-x')^2} \frac{x_U + x'_U}{2\sqrt{x_U x'_U}} \\
& - \int_0^{1-x} dy' \frac{\psi_{s_1, s_2}(x, y', \vec{e}_i)}{(y-y')^2} \frac{y_U + y'_U}{2\sqrt{y_U y'_U}}
\end{aligned} \tag{2.5}$$

In Eq. (2.4), the first two terms on the right hand side are the kinetic energies of the quark and the anti-quark while the third term describes the Coulomb interaction between them. In Eq. (2.5), the first three terms on the right hand side are the kinetic energies of the quark, anti-quark and the link fields, the fourth term describes the Coulomb interaction between the quark(antiquark) and the link field and the fifth term describes the Coulomb interaction between the antiquark(quark) and the link field. It should be noted that a Coulomb interaction term between the quark and antiquark in the 3-particle sector does not appear since it is disallowed under the large N_c limit. Three remarks are in order at this point. First, H_{22} and H_{33} , i.e. the terms in the Hamiltonian that are diagonal in Fock space are independent of the quark spin and the orientation of the link. Second, the ψ 's in Eqs. (2.4) and (2.5) still depend implicitly on k_\perp because although k_\perp is conserved, k_\perp still enters the integral equations as a parameter. Finally, Eqs. (2.4) and (2.5) have been rescaled in a manner such that $G^2 = 1$.

The natural question that arises at this point is: How do the 2-sector and the 3-sector mix with each other. This brings us to the issue of propagation of the mesons on the lattice. Qualitatively, the way this takes place is as follows: A $q(\bar{q})$ hops to a neighboring site with the emission of a link field (2-sector \rightarrow 3-sector). The $\bar{q}(q)$ sitting on the original site then jumps to join the $q(\bar{q})$ by absorbing the link field (3-sector \rightarrow 2-sector). Since this propagation resembles that of an inchworm on a scale of a femtometer, we were inspired to call this the *femtoworm approximation*. The hopping of a quark or an antiquark from one site to the next can cause it to either flip its spin or not. Accordingly, we introduce two distinct couplings between the fermion and the link degrees of freedom. In this work, we label the spin-flip coupling as m_v and the non spin-flip coupling as m_r . The corresponding interaction terms

are presented in details later in this section. The natural question that now arises from the above is: Is it possible for a link field that is emitted by a quark(antiquark) through the m_r coupling to be absorbed by an antiquark(quark) through the m_v term, in other words, ‘mixed’ hopping ? The answer to this is ‘No’. To understand the hopping interactions better one needs to analyze the rotational properties of the Hamiltonian more closely. For $\mathbf{k}_\perp = 0$, the \perp lattice Hamiltonian is invariant under rotations around the z – *axis* by multiples of $\pi/2$, giving rise to conservation of total angular momentum modulo 4. Since $J_z = S_z$ in the 2 particle sector and S_z can only assume the values $-1, 0$, and 1 , S_z in the 2 particle sector is conserved. Since mixed hopping would change S_z by one unit, this means that the sum of all contributions from mixed hopping must add up to zero. The observation that helicity conservation (modulo 4) for $\vec{k}_\perp = 0$ prohibits interference between the two hopping terms was already made in Ref. [8].

The interaction of the 2-particle sector with the 3-particle sector will therefore have four different possibilities:

- a quark(or an antiquark) in the 2-sector emits a link through the m_v term and flips it’s spin.
- a quark(or an antiquark) in the 2-sector emits a link through the m_r term and does not flip it’s spin.

Of course, the interaction to go from the 3-sector to the 2-sector has the opposite effect, i.e,

- a quark(or an antiquark) in the 3-sector absorbs a link through the m_v term and flips it’s spin.
- a quark(or an antiquark) in the 3-sector absorbs a link through the m_r term and does not flip it’s spin.

In order to understand the spin dynamics due to the hopping terms as described above we present below the interaction Hamiltonian in all its glory.

Spin flip hopping in the x -direction:

$$\begin{aligned}
\delta H_x^{flip} = & \tag{2.6} \\
& -i \left(\frac{m_v}{p_f^+} - \frac{m_v}{p_i^+} \right) \sum_{\vec{n}_\perp} [b_\uparrow^\dagger(\vec{n}_\perp, p_f^+) b_\downarrow(\vec{n}_\perp + \vec{e}_x, p_i^+) \\
& \quad - b_\downarrow^\dagger(\vec{n}_\perp, p_f^+) b_\uparrow(\vec{n}_\perp + \vec{e}_x, p_i^+) \\
& \quad - b_\uparrow^\dagger(\vec{n}_\perp, p_f^+) b_\downarrow(\vec{n}_\perp - \vec{e}_x, p_i^+) \\
& \quad + b_\downarrow^\dagger(\vec{n}_\perp, p_f^+) b_\uparrow(\vec{n}_\perp - \vec{e}_x, p_i^+) \\
& \quad - d_\uparrow^\dagger(\vec{n}_\perp, p_f^+) d_\downarrow(\vec{n}_\perp + \vec{e}_x, p_i^+) \\
& \quad + d_\downarrow^\dagger(\vec{n}_\perp, p_f^+) d_\uparrow(\vec{n}_\perp + \vec{e}_x, p_i^+) \\
& \quad + d_\uparrow^\dagger(\vec{n}_\perp, p_f^+) d_\downarrow(\vec{n}_\perp - \vec{e}_x, p_i^+) \\
& \quad - d_\downarrow^\dagger(\vec{n}_\perp, p_f^+) d_\uparrow(\vec{n}_\perp - \vec{e}_x, p_i^+)]
\end{aligned}$$

Spin flip hopping in the y -direction:

$$\begin{aligned}
\delta H_y^{flip} = & \tag{2.7} \\
& - \left(\frac{m_v}{p_f^+} - \frac{m_v}{p_i^+} \right) \sum_{\vec{n}_\perp} [b_\uparrow^\dagger(\vec{n}_\perp, p_f^+) b_\downarrow(\vec{n}_\perp + \vec{e}_y, p_i^+) \\
& \quad + b_\downarrow^\dagger(\vec{n}_\perp, p_f^+) b_\uparrow(\vec{n}_\perp + \vec{e}_y, p_i^+) \\
& \quad - b_\uparrow^\dagger(\vec{n}_\perp, p_f^+) b_\downarrow(\vec{n}_\perp - \vec{e}_y, p_i^+) \\
& \quad - b_\downarrow^\dagger(\vec{n}_\perp, p_f^+) b_\uparrow(\vec{n}_\perp - \vec{e}_y, p_i^+) \\
& \quad - d_\uparrow^\dagger(\vec{n}_\perp, p_f^+) d_\downarrow(\vec{n}_\perp + \vec{e}_y, p_i^+) \\
& \quad - d_\downarrow^\dagger(\vec{n}_\perp, p_f^+) d_\uparrow(\vec{n}_\perp + \vec{e}_y, p_i^+) \\
& \quad + d_\uparrow^\dagger(\vec{n}_\perp, p_f^+) d_\downarrow(\vec{n}_\perp - \vec{e}_y, p_i^+) \\
& \quad + d_\downarrow^\dagger(\vec{n}_\perp, p_f^+) d_\uparrow(\vec{n}_\perp - \vec{e}_y, p_i^+)]
\end{aligned}$$

Hopping without spin flip:

$$\begin{aligned}
\delta H^{no-flip} = & \tag{2.8} \\
& - \left(\frac{m_r}{p_f^+} + \frac{m_r}{p_i^+} \right) \sum_{\vec{n}_\perp} [b_\uparrow^\dagger(\vec{n}_\perp, p_f^+) b_\uparrow(\vec{n}_\perp + \vec{e}_x, p_i^+)
\end{aligned}$$

$$\begin{aligned}
& +b_{\uparrow}^{\dagger}(\vec{n}_{\perp}, p_f^+)b_{\uparrow}(\vec{n}_{\perp} - \vec{e}_x, p_i^+) \\
& +b_{\downarrow}^{\dagger}(\vec{n}_{\perp}, p_f^+)b_{\downarrow}(\vec{n}_{\perp} + \vec{e}_x, p_i^+) \\
& +b_{\downarrow}^{\dagger}(\vec{n}_{\perp}, p_f^+)b_{\downarrow}(\vec{n}_{\perp} - \vec{e}_x, p_i^+) \\
& +d_{\uparrow}^{\dagger}(\vec{n}_{\perp}, p_f^+)d_{\uparrow}(\vec{n}_{\perp} + \vec{e}_x, p_i^+) \\
& +d_{\uparrow}^{\dagger}(\vec{n}_{\perp}, p_f^+)d_{\uparrow}(\vec{n}_{\perp} - \vec{e}_x, p_i^+) \\
& +d_{\downarrow}^{\dagger}(\vec{n}_{\perp}, p_f^+)d_{\downarrow}(\vec{n}_{\perp} + \vec{e}_x, p_i^+) \\
& +d_{\downarrow}^{\dagger}(\vec{n}_{\perp}, p_f^+)d_{\downarrow}(\vec{n}_{\perp} - \vec{e}_x, p_i^+) \\
& +b_{\uparrow}^{\dagger}(\vec{n}_{\perp}, p_f^+)b_{\uparrow}(\vec{n}_{\perp} + \vec{e}_y, p_i^+) \\
& +b_{\uparrow}^{\dagger}(\vec{n}_{\perp}, p_f^+)b_{\uparrow}(\vec{n}_{\perp} - \vec{e}_y, p_i^+) \\
& +b_{\downarrow}^{\dagger}(\vec{n}_{\perp}, p_f^+)b_{\downarrow}(\vec{n}_{\perp} + \vec{e}_y, p_i^+) \\
& +b_{\downarrow}^{\dagger}(\vec{n}_{\perp}, p_f^+)b_{\downarrow}(\vec{n}_{\perp} - \vec{e}_y, p_i^+) \\
& +d_{\uparrow}^{\dagger}(\vec{n}_{\perp}, p_f^+)d_{\uparrow}(\vec{n}_{\perp} + \vec{e}_y, p_i^+) \\
& +d_{\uparrow}^{\dagger}(\vec{n}_{\perp}, p_f^+)d_{\uparrow}(\vec{n}_{\perp} - \vec{e}_y, p_i^+) \\
& +d_{\downarrow}^{\dagger}(\vec{n}_{\perp}, p_f^+)d_{\downarrow}(\vec{n}_{\perp} + \vec{e}_y, p_i^+) \\
& +d_{\downarrow}^{\dagger}(\vec{n}_{\perp}, p_f^+)d_{\downarrow}(\vec{n}_{\perp} - \vec{e}_y, p_i^+)]
\end{aligned}$$

Implicit in the above expressions are link field creation and annihilation operators on the link connecting the initial and final state.

The transition matrix elements are obtained by sandwiching the above interactions between the 2-particle and the 3-particle states as written in Eqs. (2.2) and (2.3) and are provided in the table in appendix B.

The schematic structure of the Hamiltonian therefore looks like the following:

$$H \begin{bmatrix} \psi(x) \\ \psi(x, y) \end{bmatrix} = \begin{bmatrix} H_{22} & H_{23} \\ H_{32} & H_{33} \end{bmatrix} \begin{bmatrix} \psi(x) \\ \psi(x, y) \end{bmatrix} \quad (2.9)$$

where H_{23} and H_{32} involve all the transition matrix elements.

In order to evaluate all the matrix elements, we expanded the wavefunction amplitudes using a basis of continuous functions as follows:

$$\psi(x) = \sum_{k=0}^{\Lambda} k x^{\beta+k} (1-x)^{\beta} \quad (2.10)$$

$$\psi(x, y) = \sum_{k=0}^{\Lambda} \sum_{l=0}^{\Lambda-k} a_{kl} x^{\beta+k} y^{\beta+l} (1-x-y)^{\beta+\frac{1}{2}} \quad (2.11)$$

where the Λ in the Eq. 2.10 and that in Eq. 2.11 need not be equal.

In the table (see appendix B), $F_q^r(F_{\bar{q}}^r)$ are the overlap integrals when a quark(antiquark) in the 2-sector goes to the 3-sector by emitting a link field through the m_r hopping term (the spin non-flip term) and $f_q(f_{\bar{q}})$ are the overlap integrals when a quark(antiquark) in the 2-sector goes to the 3-sector by emitting a link field through the m_v hopping term (the spin-flip term). See appendix A for more details of these overlap integrals.

A factor $\left(\frac{x'}{x}\right)^{\epsilon}$ was introduced in the integrand of the transition matrix elements to regularize the infrared (small x, x') divergence that arises from the self energy of quarks in the case when the quark that emits a link field also absorbs it. Of course, all physical observables will have to be independent of the value of ϵ as will be demonstrated in section IV.

The result of all the above is the following matrix equation for each k and k, l :

$$H \begin{bmatrix} N_{k,k'} & 0 \\ 0 & N_{kl,k'l'} \end{bmatrix} \begin{bmatrix} a_{k'} \\ a_{k'l'} \end{bmatrix} = \begin{bmatrix} M_{kk'} & M_{k,k'l'} \\ M_{k'l',k} & M_{kl,k'l'} \end{bmatrix} \begin{bmatrix} a_{k'} \\ a_{k'l'} \end{bmatrix} \quad (2.12)$$

where $N_{k,k'}$ and $N_{kl,k'l'}$ are the norm matrices, $M_{kk'}$ and $M_{kl,k'l'}$ are the matrix elements in the pure 2-particle and 3-particle sectors, respectively and finally $M_{k,k'l'}$ and $M_{k'l',k}$ are the transition matrix elements. The above matrix equation is then converted into an eigenvalue equation that yields eigenvectors in terms of the a_k 's and a_{kl} 's.

Another significant result of this approximation that is worth mentioning at this point is that unlike the low lying mesons, the higher excited states are not expected to show the correct dispersion. The reason for this is that since the higher states are very excited, the quark and the antiquark will be physically farther apart. This would mean that these mesons will mostly or always remain in the $q\bar{q}U$ (where U is the link field) state (see Fig. 3) and for it to propagate, it will need to go to a $q\bar{q}UU$ state or states with larger number of link fields. But since our approximation does not allow states with more than one link field, these excited states simply cannot propagate.

III. PERTURBATIVE ANALYSIS OF THE π - ρ SPLITTING

In order to gain a qualitative understanding about the interplay between different parameters in the \perp lattice Hamiltonian, it is instructive to study a simple model, where one treats the admixture of the 3-particle Fock component to the π and ρ as a perturbation.

To 0^{th} order, i.e. when the coupling between 2 and 3 particle Fock component is turned off, there is no spin dependence of the interactions and the π and ρ are degenerate. Likewise, there is no ‘hopping’ (i.e. \perp propagation) of mesons and thus energies are independent of \mathbf{k}_\perp giving rise to an infinite \perp lattice spacing (in physical units).

In the next order we treat the coupling between 2 and 3 particle Fock components as a perturbation (note that interactions which are diagonal in the particle number, such as the confining interaction in the longitudinal direction are still treated non-perturbatively). As described in section II, there are two interactions that mix Fock sectors: hopping due to the m_r -term (without helicity flip) and hopping due to the vector coupling m_v (with helicity flip). Starting from a basis of ‘t Hooft eigenstates which are plane waves in the \perp direction and where the $q\bar{q}$ in the 2 particle Fock component carry spins $|\uparrow\uparrow\rangle$, $|\uparrow\downarrow\rangle$, $|\downarrow\uparrow\rangle$, and $|\downarrow\downarrow\rangle$ respectively, one thus finds for the energy in second order perturbation theory to be:

$$\begin{aligned}
H = M_0^2 - M_{1,r}^2 & \begin{pmatrix} c_x + c_y & 0 & 0 & 0 \\ 0 & c_x + c_y & 0 & 0 \\ 0 & 0 & c_x + c_y & 0 \\ 0 & 0 & 0 & c_x + c_y \end{pmatrix} \\
+ M_{1,v}^2 & \begin{pmatrix} 0 & 0 & 0 & c_y - c_x \\ 0 & 0 & c_x + c_y & 0 \\ 0 & c_x + c_y & 0 & 0 \\ c_y - c_x & 0 & 0 & 0 \end{pmatrix}.
\end{aligned} \tag{3.1}$$

Here $M_{1,r}^2$ and $M_{1,v}^2$ are some second order perturbation theory expressions involving matrix elements between 2 and 3 particle states that are eigenstates of the diagonal parts of the Hamiltonian (kinetic + Coulomb), and $c_i \equiv \cos k_i$.

Several general and important features can be read off from this result. First of all, and most importantly, Eq. (3.1) shows that the r-term gives rise to a dispersion relation with the same \perp speed of light for the π and the ρ 's, while the vector interaction breaks that symmetry. This observation already indicates that it may be desirable to keep the r -term much larger than the spin-flip term. We will elaborate on this point below.

At $k_x = k_y = 0$, the eigenstates of the above Hamiltonian are the $\rho_{\pm 1}$ i.e. $|\uparrow\uparrow\rangle$ and $|\downarrow\downarrow\rangle$, with $M^2 = M_{\pm 1}^2 \equiv M_0^2 - M_{1,r}^2$, the $|\rho_0\rangle \equiv |\uparrow\downarrow + \downarrow\uparrow\rangle$, with $M^2 = M_{\pm 1}^2 + M_{1,v}^2$ and the $|\pi\rangle \equiv |\uparrow\downarrow - \downarrow\uparrow\rangle$, with $M^2 = M_{\pm 1}^2 - M_{1,v}^2$. For nonzero \perp momenta, there will in general be mixing among the ρ_{+1} and the ρ_{-1} , but not among the other states since helicity in the 2-particle Fock sector is still conserved modulo 2. Expanding around $\mathbf{k}_\perp = 0$, and denoting $\bar{M}^2 \equiv M_0^2 - M_{1,r}^2$ one finds to $\mathcal{O}(\mathbf{k}_\perp^2)$ the following eigenstates and eigenvalues.

state	$M^2(0)$	$M^2(\mathbf{k}_\perp^2) - M^2(0)$
$\uparrow\downarrow - \downarrow\uparrow$	$\bar{M}^2 - M_{1,v}^2$	$M_{1,r}^2 \frac{k_x^2 + k_y^2}{2} + M_{1,v}^2 \frac{k_x^2 + k_y^2}{2}$
$\uparrow\downarrow + \downarrow\uparrow$	$\bar{M}^2 + M_{1,v}^2$	$M_{1,r}^2 \frac{k_x^2 + k_y^2}{2} - M_{1,v}^2 \frac{k_x^2 + k_y^2}{2}$
$\uparrow\uparrow - \downarrow\downarrow$	\bar{M}^2	$M_{1,r}^2 \frac{k_x^2 + k_y^2}{2} - M_{1,v}^2 \frac{k_x^2 - k_y^2}{2}$
$\uparrow\uparrow + \downarrow\downarrow$	\bar{M}^2	$M_{1,r}^2 \frac{k_x^2 + k_y^2}{2} + M_{1,v}^2 \frac{k_x^2 - k_y^2}{2}$

(3.2)

Eq. (3.2) illustrates a fundamental dilemma that hampers any attempt to fully restore Lorentz invariance within the femtoworm approximation: $M_{1,v}^2$ not only governs the splitting between the π and the ($h=0$) ρ but is also responsible for violations of Lorentz invariance among the different helicity states: If one determines the \perp lattice spacing in physical units for each meson separately, by demanding that the \perp speed of light equals 1, one finds for example

$$\begin{aligned}
\left. \frac{1}{a_\perp^2} \right|_\pi &= M_{1,r}^2 + M_{1,v}^2 \\
\left. \frac{1}{a_\perp^2} \right|_{\rho_0} &= M_{1,r}^2 - M_{1,v}^2
\end{aligned}
\tag{3.3}$$

i.e. increasing the π - ρ splitting is typically accompanied by an increase in Lorentz invariance violation

$$\left. \frac{1}{a_\perp^2} \right|_\pi - \left. \frac{1}{a_\perp^2} \right|_\rho = M_{\rho_0}^2 - M_\pi^2.
\tag{3.4}$$

For the $\rho_{\pm 1}$ the breaking is of a similar scale, plus one also observes an anisotropy in the dispersion relation on the same scale.

Therefore, in order to avoid a large breaking of Lorentz invariance, it will be necessary that

$$M_{r,1}^2 \gg M_{\rho_0}^2 - M_\pi^2.
\tag{3.5}$$

If one keeps the $\pi - \rho$ splitting fixed at its physical value then there are two ways to achieve this condition. One possibility is to simply increase the Yukawa coupling that appears in the r -term. This increase of the r -term tends to decrease the \perp lattice spacing for both π and ρ 's (see Fig. 2) and in order to achieve satisfactory Lorentz invariance (in the sense of uniform \perp lattice spacings) one needs to make the lattice spacing smaller than the Compton wavelength of the ρ meson. However, one cannot make the r -term coupling arbitrarily large because at some point there occurs an instability (tachyonic $M^2!$). Such instabilities for large coupling are common in the LF formulation of models with Yukawa coupling and might be related to a phase transition (similar to the phase transition in ϕ^4 theory that occurs as the coupling is increased).

Fortunately, there exists another possibility to make these matrix elements large, without increasing the Yukawa couplings. This derives from the fact that the hopping interactions are proportional to $\left(\frac{1}{x} \pm \frac{1}{x'}\right) \frac{1}{x-x'}$, where x (x') are the momenta of the active quark before(after) the hopping. Because of the singularity as $x, x' \rightarrow 0$, matrix elements of the hopping terms are greatly enhanced if the unperturbed wave functions are large near $x = 0$ and $x = 1$. Since the unperturbed wave functions in the 2 particle Fock component vanish like x^β near $x = 0$, where $\beta \propto \frac{G}{m_q}$, matrix elements of the hopping interaction become very large when one makes $\frac{G^2}{m_q^2}$ very large.

Therefore, the larger one chooses $\frac{G^2}{m^2}$, the more one restores Lorentz invariance of the π and ρ dispersion relations because one can keep the π - ρ splitting fixed while decreasing the coupling of the spin flip interaction. At the same time, keeping the r -term interaction fixed one increases the dominance of the r -term contribution in $\frac{1}{a^2}$ and thus not only reduces the lattice spacing in physical units, but also obtains dispersion relations for the π and the ρ 's that look more and more similar — as demanded by Lorentz invariance. Unfortunately, we are not completely free to pick whatever value of $\frac{G^2}{m_q^2}$ we like because m_q^2 and G^2 are largely fixed by the center of mass in the π - ρ system as well as by fitting the physical string tension in the pure glue sector.

The above analysis may also shed some light on the shape of the pion distribution

amplitude in Ref. [9], which is much more flat (actually, it even exhibits a slight double-hump shape) compared to our results (see next section). The reason is that the numerical value for G^2 in Ref. [9] was *not* taken from the pure glue calculation, but was rather used as a free parameter, which was also varied in order to maximize Lorentz covariance. Although such a *first principle* approach would normally be desirable, minimizing Lorentz covariance violations for the π and ρ dispersion relations drives $G^2 \rightarrow \infty$. When the longitudinal gauge coupling G^2 is very large compared to other scales in the problem, the wavefunction tends to become very flat — a phenomenon familiar from the 't Hooft equation. Of course, since a DLCQ cutoff was employed in Ref. [9], G^2 never really become infinite, but through the extrapolation procedure the near flat shape for the pion distribution amplitude emerged. In a more recent paper [11], where Dalley adopted a procedure similar to ours and G^2 was kept fixed, a pion distribution amplitude is obtained that is much more consistent with ours.

IV. NONPERTURBATIVE NUMERICAL RESULTS

One cannot expect this Hamiltonian to describe the higher excited states because of the truncation of the Fock space upto the 3-particle sector. This is demonstrated in Fig. 3 where we show typical results for the probability to find each state to be in the 3-particle sector. One finds that whereas the low-lying states have a fairly large probability to be in the 2-particle sector, it is quite the opposite for the higher states. We therefore expect that excited states are much more strongly affected by the omission of 4 and more particle states and consider in the following only the π and ρ states in our study of Lorentz covariance.

The parameters in the Hamiltonian are:

- longitudinal gauge coupling
- r -term coupling (hopping without spin flip)
- spin-flip coupling (hopping with spin flip)
- kinetic mass (2 particle sector)

- kinetic mass (3 particle sector). The observables that we studied showed little dependence on this parameter, so we kept it fixed at a constituent mass.
- link field mass. Similar to kinetic mass in 3 particle sector. Furthermore, demanding Lorentz invariance in the pure glue sector, one finds a renormalized trajectory. This makes sense since the \perp lattice scale is unphysical. We keep the link field mass fixed at a value which yields relatively small \perp lattice spacing.

In the spirit of the color-dielectric approach [7], we would like to use only chiral symmetry (small pion mass), Lorentz invariance and one length scale (e.g. physical ρ mass or string tension) as the only input into our calculations. However, as explained in the previous section, if one uses as input only the π and ρ masses, demanding exact Lorentz invariance within the framework of the femtoworm approximation would drive G^2/m_ρ^2 to infinity and would thus give rise to string tensions that are inconsistent with phenomenology. Likewise, as input only the π mass together with Lorentz invariance would give rise to a degenerate π - ρ system. It is thus clear that, as long as one does not go beyond a truncation of the Fock space above 3 particles (q , \bar{q} and one link quantum), a first principle calculation (where only one mass scale is used as input) will not be possible. In the following, we will therefore use two phenomenological scales as input parameters: the physical value of the ρ mass, as well as the physical string tension.

Although the dependence of physical parameters on the input parameters is in general rather complex and non-perturbative, one can understand at a qualitative level how the input parameters influence the relevant physical scales: The physical string tension in the longitudinal direction determines G^2 in physical units.

Modulo mass renormalization due to the Yukawa couplings, the quark mass in the 2-particle Fock component and the gauge coupling are strongly constrained by fitting the physical string tension (which determines G^2 and the center of mass of the π - ρ system. This leaves us with only the r -term and the helicity flip hopping term couplings as parameters to vary. The helicity flip term is not only responsible for π - ρ splitting within our approximations

but also for violations of Lorentz invariance (different \perp lattice spacings in physical units for different mesons).

The observables that we studied, including Lorentz invariance, show rather little sensitivity ¹ to the precise values of the 3-particle sector quark masses (Fig. 4), which we thus keep at a value corresponding to a constituent mass (about half the ρ mass). This leaves us with 4 free parameters.

Using a value of $G^2 \equiv \frac{g^2 N_C}{2\pi} \approx 0.4 \text{ GeV}^2$ in physical units, as determined from the string tension in Ref. [7] (which is larger than the one previously used [8,10]), we were able to produce the physical π - ρ splitting with only a relatively small spin-flip coupling. This allows us to chose the r -term large enough so that r -term hopping dominates over spin-flip hopping and therefore violations of Lorentz invariance (as measured by comparing quadratic terms in the dispersion relation of mesons in the π - ρ sector) are only on the order of 20%. The average \perp lattice spacing (from the dependence of the energy on \mathbf{P}_\perp) is found to be $a_\perp \approx 0.5 fm$. For the π wave function, we find a shape (see Fig. 5) that is very close to the asymptotic shape $\phi_{asy}(x) = 6x(1-x)$.

This is surprising if one considers that the lattice spacing is still relatively large and hence the momentum scale is still very low. The ρ meson distribution functions are shown in Figs. 6 and 7. Notice that the momentum dependence of the π dispersion relation is stronger than the one for the ρ and for the parameters used in our calculations this even leads to a level crossing ² The reason for this behavior is very simple. As pointed out in Ref. [8], for $\vec{k}_\perp = 0$ spin-flip hopping is attractive for the π and repulsive for the ρ_0 , while the opposite is true at the end of the Brillouin zone. More precisely, for $k_x = 0$, the hopping term in the x direction is attractive for the π and repulsive for the ρ^0 with the opposite being true for $k_x = \pi$. An analogous statement holds for the y -direction. If there were no

¹As long as we kept the other parameters floating!

²Note that there is no mixing at the crossover point since the π and ρ have opposite C-parity.

r -term present, the dispersion would arise solely from the spin flip term and the ρ_0 in the corner of the Brillouin zone would be degenerate with the π at $\vec{k}_\perp = 0$ — a phenomenon which is nothing but a manifestation of species doubling at the hadronic level. Of course, since we have included an r -term, the ρ^0 in the corner of the Brillouin zone is no longer degenerate with the π at $\vec{k}_\perp = 0$, but the level crossing remains (see Fig. 8).

Similarly one can understand the degeneracy of the π and ρ^0 at the edge of the Brillouin zone $\vec{k}_\perp = (\pi, 0)$. At that point, the x -hopping term is repulsive for the π and attractive for the ρ^0 . The opposite is true for the y -hopping term and the two contributions cancel one another leaving the π and the ρ^0 degenerate.

From the normalization of the π distribution function we were able to extract a numerical estimate for the π decay constant $f_\pi p^\mu = \langle 0 | A^\mu | p \rangle$ in terms of the $+-$ helicity component of the π wavefunction in the two particle Fock component $\Phi_{+-}(x)$

$$f_\pi = \frac{2}{a_\perp} \sqrt{\frac{N_C}{\pi}} \int_0^1 dx \psi_{+-}(x) \approx 300 \text{ MeV}, \quad (4.1)$$

which is much larger than the experimental value $f_\pi^{exp} \approx 93 \text{ MeV}$. We expect that including higher Fock components will reduce the size of the two particle Fock component and hence also f_π .

The parton distribution function for the π is shown in Fig. 10. The fact that $q(x)$ goes to zero at small x is an artifact of our ϵ -cutoff and we expect a nonzero value for $q(0)$ in the femtoworm approximation as $\epsilon \rightarrow 0$.

Finally, we also calculated the electro-magnetic form factor for the π for purely transverse momentum transfers (where overlap formulas can be used) and we find an rms radius for the π of $r_\pi^2 \equiv -6 \frac{d}{dQ^2} F(Q^2) |_{Q=0} \approx (0.243 \text{ fm})^2$. Obviously, since our lattice spacing is only about 0.5 fm and since we do not let the quark-antiquark separation to exceed one lattice unit, one should not expect very good results for this observable. Since the rms-radius is already poor, displaying the form factor is not very meaningful.

As mentioned in section II, physical observables should be independent of the infrared cut-off, ϵ (as long as the cutoff is small). We verified this cut-off independence for a variety

of observables. As an example, we demonstrate in Fig. 9 the cutoff independence of the dispersion relations for light mesons. The dashed line is for $\epsilon = 0.05$ and the continuous line is for $\epsilon=0.1$.

V. COMMENTS AND COMPARISONS

We feel it is worthwhile to compare our results with those in a concurrent paper [11] that appeared as we were completing the manuscript for this paper. There are a few noteworthy technical differences between the two. Firstly, the treatment of the longitudinal dynamics are different (DLCQ in Ref. [11] while we employed continuous basis functions). Secondly, the pure glue string tension are different ($\sim \frac{2}{3} fm$ vs. $\sim 0.5 fm$) Otherwise, both this work and Ref. [11] were based on the formalism outlined in Ref. [8].

We used continuous basis functions because there are some unresolved issues regarding the convergence of DLCQ calculations in terms of the DLCQ resolution [13]. However, because the numerical approximations in both works are very crude, these issues are not yet very important and therefore the main difference in this context is more in calculational details.

Because both works used the femtoworm approximation, the rms radius of the π is rather low compared to the experimental value. The lattice spacing, which defines the maximal $q\bar{q}$ -separation, is slightly larger in Ref. [11]. Consequently, the resulting rms radius in Ref. [11], though still much smaller than the experimental result, is slightly larger than ours.

Here we should also point out that the algebraic expression used in Ref. [11] for calculating f_π is incorrect. With our normalization, the result for f_π in Ref. [11] increases by a factor of three [15] and becomes much more similar to ours.

Since both works determine the parameters in the effective theory by imposing Lorentz symmetry as a nonperturbative renormalization condition, we feel that it is important to have a handle on the violation of Lorentz invariance (or lack thereof) within the femtoworm approximation. That this violation is inevitable was first pointed out in Ref. [14] (in which

some results from this work were already presented) and has been further reiterated in section III of this paper. Since it is impossible to achieve both Lorentz invariance and the correct $\pi - \rho$ splitting simultaneously, one, therefore, needs to have a quantitative idea of the degree to which Lorentz invariance can be achieved while simultaneously yielding the correct $\pi - \rho$ splitting. Although Ref. [11] provides several χ^2 plots, it is not quantitatively clear from these plots how large the violations of Lorentz invariance are for the $\pi - \rho$ dispersion relations at the minimum of χ^2 . It is therefore not possible for us to compare the two works with respect to the degree to which Lorentz symmetry is violated. Here we should also point out an interesting connection between this work and Ref. [11] on the one hand and Ref. [8] on the other: although the spirit of Ref. [8] was more phenomenological³, the final results (parton distribution functions, distribution amplitudes) obtained in Ref. [8] were very similar to both Ref. [11] and this work.

Another difference between our results and those in Ref. [11] is that our π distribution amplitude is closer to the ‘asymptotic’ shape than the one in Ref. [11] — a behavior which is also reflected in the parton distribution function. However, this difference is not really significant and it may just be due to the differences in the handling of the longitudinal dynamics which may favor slightly different sets of parameters.

VI. SUMMARY AND CONCLUSIONS

We presented results from a study of light mesons in QCD formulated on a transverse lattice using light-front quantization. In transverse lattice QCD the gauge field in the (continuous) longitudinal directions is described by a non-compact vector potential, and in the (discrete) transverse directions by a non-compact link field. Our approach was based on

³The quark mass in the three particle Fock component in Ref. [8] was simply taken to be a constituent mass rather than being fitted to optimize Lorentz symmetry and the ratio of the flip to nonflip coupling was simply kept fixed in the fit of mass spectra.

the color-dielectric formulation [7], where one assumes that the fields have been “smeared” over a finite area and thus are no longer subject to a strict $SU_C(N)$ constraint.

The smeared degrees of freedom are subject to effective interactions which reflect the dynamics of the underlying microscopic degrees of freedom. Although this effective interaction is not known *a priori*, it is highly constrained because it must still be gauge invariant and it should still give rise to Lorentz invariant observables. In this work we investigated transverse lattice QCD with fermions. The starting point was an ansatz for the effective interactions which contained interaction terms up to fourth order in the fields which are still invariant under those symmetries not broken by the transverse lattice. The goal of this work was to determine the coefficients in this ansatz by demanding enhanced Lorentz symmetry from physical observables. As input parameters we used the physical masses of the π and the ρ as well as the string tension. What we found is that the splitting between the π and ρ mesons strongly constrains the quark helicity flip interaction term in the LF-Hamiltonian. Meson propagation in the \perp direction involves helicity flip and nonflip hopping terms for the quarks. Once the nonflip hopping term was constrained by fitting the observed $\pi - \rho$ splitting, the only remaining parameter on which the physical lattice spacing (as determined from the meson dispersion relation) depends very strongly is the helicity nonflip term. Even though we scanned the parameter space thoroughly, we were only able to find matching values for a_\perp for the π and ρ mesons within about a 10% - 20% error. Similar Lorentz invariance violations were found in the splitting between ρ mesons of helicity zero and one. We believe that both these errors are due to the truncation of the Fock space (which may contain an infinite number of particles) as well as the ansatz for the effective interaction (which may contain an infinite number of terms). In fact, given these rather crude approximations, it is actually remarkable that the violations of Lorentz invariance in the light meson sector are only about 10-20% . The model seems very promising though it displays some basic limitations as far as restoration of full Lorentz invariance is concerned. This problem was first identified in one of our earlier papers [10] but subsequent new understanding [12] about the couplings helped isolate the problem and reduce it significantly for the low-lying mesons.

For the higher mesons, the femtoworm approximation is not expected to work unless more link field degrees of freedom are introduced, a task that is possible but computationally non-trivial.

While we were completing this work, similar studies of mesons on the transverse lattice appeared [9,11], which were based on DLCQ rather than basis function techniques for handling the longitudinal dynamics. However, there is another important difference between our work and Ref. [9]: we took the numerical value for the longitudinal gauge coupling G that was obtained in pure glue studies on the \perp lattice [7], while Ref. [9] allowed G to ‘float’ in addition to the other parameters in order to restore Lorentz symmetry. As we explained in Section III, increasing G , as compared to other dimensionful parameters, tends to decrease violations of Lorentz symmetry in the π/ρ dispersion relations. Therefore, the results presented in Ref. [9] were extrapolated from calculations performed with values of G that were much larger than ours (and larger than G used in the pure glue calculation in Ref. [7]). This difference in *procedure* explains to some extent the difference in Results between this work and Refs. [9]: most importantly, if one increases G in physical units, while keeping the physical pion mass fixed, tends to decrease all other dimensionful parameters ⁴. The pion distribution amplitudes presented in Ref. [9], where G was allowed to float completely freely, although slightly ‘double humped’, is actually numerically consistent with an almost completely flat distribution since it was obtained by extrapolation in the DLCQ parameter and there is some uncertainty in this procedure, and this is consistent with the above observation regarding G . In Ref. [11], G was no longer allowed to float and the results for the distribution amplitude are much more similar to ours.

Acknowledgments M.B. would like to thank S. Dalley for many interesting and clarifying discussions about the \perp lattice. This work was supported by a grant from DOE (FG03-

⁴One can understand this fact by comparing with the simpler but similar 1+1 dimensional ‘t Hooft model

95ER40965) and through Jefferson Lab by contract DE-AC05-84ER40150 under which the Southeastern Universities Research Association (SURA) operates the Thomas Jefferson National Accelerator Facility.

APPENDIX A: OVERLAP INTEGRALS

To understand the overlap integrals, let us look at two specific elements of the table (see appendix B), namely, the first two elements of the first row. For the first element, clearly there is no spin flip and the hopping is along the y -direction. There are two possibilities through which this transition can take place. Pictorially, they are as shown in Fig. 11.

Notice that both diagrams yield the same 3-sector lattice configuration which is shown to the right. These two diagrams correspond to the terms containing $b_{\uparrow}^{\dagger}(\vec{n}_{\perp}, p_f^+)b_{\uparrow}(\vec{n}_{\perp} - \vec{e}_y, p_i^+)$ and $d_{\uparrow}^{\dagger}(\vec{n}_{\perp}, p_f^+)d_{\uparrow}(\vec{n}_{\perp} + \vec{e}_y, p_i^+)$ in the the spin non-flip interaction Hamiltonian. When these two terms are sandwiched between $|qq\rangle$ and $|qqg\rangle$ from eqns. 2.2 and 2.3, one obtains the first matrix element of the table. In particular, F_q^r and $F_{\bar{q}}^r$ are obtained when the integrals over the quark and the antiquark momenta are carried out in the above matrix element as follows:

$$F_q^r = \int dx \int dy \psi^*(x, y) \left(\frac{m_r}{x} + \frac{m_r}{1-y} \right) \frac{1}{\sqrt{1-x-y}} \psi(1-y) \quad (\text{A1})$$

$$F_{\bar{q}}^r = \int dx \int dy \psi^*(x, y) \left(\frac{m_r}{y} + \frac{m_r}{1-x} \right) \frac{1}{\sqrt{1-x-y}} \psi(x) \quad (\text{A2})$$

Similarly, let us look at the second element of the first row of the table. Clearly, this is a spin flip interaction and the hopping takes place in the y -direction. Pictorially, this is shown in Fig. 12.

This diagram corresponds to the term in δH_y^{flip} containing $d_{\uparrow}^{\dagger}(\vec{n}_{\perp}, p_f^+)d_{\downarrow}(\vec{n}_{\perp} + \vec{e}_y, p_i^+)$. The equivalent 3-sector lattice configuration is once again shown to the right. The corresponding

matrix element is therefore obtained by sandwiching this term of the Hamiltonian between $|qq\rangle$ and $|qqg\rangle$ and in particular $f_{\bar{q}}$ is obtained when the integrals over the quark and the antiquark momenta are carried out in the above matrix element as follows:

$$f_q = \int dx \int dy \psi^*(x, y) \left(\frac{m_v}{x} - \frac{m_v}{1-y} \right) \frac{1}{\sqrt{1-x-y}} \psi(1-y) \quad (\text{A3})$$

$$f_{\bar{q}} = \int dx \int dy \psi^*(x, y) \left(\frac{m_v}{y} - \frac{m_v}{1-x} \right) \frac{1}{\sqrt{1-x-y}} \psi(x). \quad (\text{A4})$$

APPENDIX B: TRANSITION MATRIX

states	$ \psi_2, \uparrow\uparrow\rangle$	$ \psi_2, \uparrow\downarrow\rangle$	$ \psi_2, \downarrow\uparrow\rangle$	$ \psi_2, \downarrow\downarrow\rangle$
$ \psi_3, \uparrow\uparrow, +\vec{e}_y\rangle$	$F_q^r e^{-\frac{ik_y}{2}} + F_{\bar{q}}^r e^{\frac{ik_y}{2}}$	$-f_{\bar{q}} e^{\frac{ik_y}{2}}$	$-f_q e^{-\frac{ik_y}{2}}$	0
$ \psi_3, \uparrow\downarrow, +\vec{e}_y\rangle$	$-f_{\bar{q}} e^{\frac{ik_y}{2}}$	$F_q^r e^{-\frac{ik_y}{2}} + F_{\bar{q}}^r e^{\frac{ik_y}{2}}$	0	$-f_q e^{-\frac{ik_y}{2}}$
$ \psi_3, \downarrow\uparrow, +\vec{e}_y\rangle$	$-f_q e^{-\frac{ik_y}{2}}$	0	$F_q^r e^{-\frac{ik_y}{2}} + F_{\bar{q}}^r e^{\frac{ik_y}{2}}$	$-f_{\bar{q}} e^{\frac{ik_y}{2}}$
$ \psi_3, \downarrow\downarrow, +\vec{e}_y\rangle$	0	$-f_q e^{-\frac{ik_y}{2}}$	$-f_{\bar{q}} e^{\frac{ik_y}{2}}$	$F_q^r e^{-\frac{ik_y}{2}} + F_{\bar{q}}^r e^{\frac{ik_y}{2}}$
$ \psi_3, \uparrow\uparrow, +\vec{e}_x\rangle$	$F_q^r e^{-\frac{ik_x}{2}} + F_{\bar{q}}^r e^{\frac{ik_x}{2}}$	$-if_{\bar{q}} e^{\frac{ik_x}{2}}$	$-if_q e^{-\frac{ik_x}{2}}$	0
$ \psi_3, \uparrow\downarrow, +\vec{e}_x\rangle$	$if_{\bar{q}} e^{\frac{ik_x}{2}}$	$F_q^r e^{-\frac{ik_x}{2}} + F_{\bar{q}}^r e^{\frac{ik_x}{2}}$	0	$-if_q e^{-\frac{ik_x}{2}}$
$ \psi_3, \downarrow\uparrow, +\vec{e}_x\rangle$	$if_q e^{-\frac{ik_x}{2}}$	0	$F_q^r e^{-\frac{ik_x}{2}} + F_{\bar{q}}^r e^{\frac{ik_x}{2}}$	$-if_{\bar{q}} e^{\frac{ik_x}{2}}$
$ \psi_3, \downarrow\downarrow, +\vec{e}_x\rangle$	0	$if_{\bar{q}} e^{-\frac{ik_x}{2}}$	$if_q e^{\frac{ik_x}{2}}$	$F_q^r e^{-\frac{ik_x}{2}} + F_{\bar{q}}^r e^{\frac{ik_x}{2}}$

states	$ \psi_2, \uparrow\uparrow\rangle$	$ \psi_2, \uparrow\downarrow\rangle$	$ \psi_2, \downarrow\uparrow\rangle$	$ \psi_2, \downarrow\downarrow\rangle$
$ \psi_3, \uparrow\uparrow, -\vec{e}_y\rangle$	$F_q^r e^{\frac{ik_y}{2}} + F_{\bar{q}}^r e^{-\frac{ik_y}{2}}$	$f_{\bar{q}} e^{-\frac{ik_y}{2}}$	$f_q e^{\frac{ik_y}{2}}$	0
$ \psi_3, \uparrow\downarrow, -\vec{e}_y\rangle$	$f_{\bar{q}} e^{-\frac{ik_y}{2}}$	$F_q^r e^{\frac{ik_y}{2}} + F_{\bar{q}}^r e^{-\frac{ik_y}{2}}$	0	$f_q e^{\frac{ik_y}{2}}$
$ \psi_3, \downarrow\uparrow, -\vec{e}_y\rangle$	$f_q e^{\frac{ik_y}{2}}$	0	$F_q^r e^{\frac{ik_y}{2}} + F_{\bar{q}}^r e^{-\frac{ik_y}{2}}$	$f_{\bar{q}} e^{-\frac{ik_y}{2}}$
$ \psi_3, \downarrow\downarrow, -\vec{e}_y\rangle$	0	$f_q e^{\frac{ik_y}{2}}$	$f_{\bar{q}} e^{-\frac{ik_y}{2}}$	$F_q^r e^{\frac{ik_y}{2}} + F_{\bar{q}}^r e^{-\frac{ik_y}{2}}$
$ \psi_3, \uparrow\uparrow, -\vec{e}_x\rangle$	$F_q^r e^{\frac{ik_x}{2}} + F_{\bar{q}}^r e^{-\frac{ik_x}{2}}$	$if_{\bar{q}} e^{-\frac{ik_x}{2}}$	$if_q e^{\frac{ik_x}{2}}$	0
$ \psi_3, \uparrow\downarrow, -\vec{e}_x\rangle$	$-if_{\bar{q}} e^{-\frac{ik_x}{2}}$	$F_q^r e^{\frac{ik_x}{2}} + F_{\bar{q}}^r e^{-\frac{ik_x}{2}}$	0	$if_q e^{\frac{ik_x}{2}}$
$ \psi_3, \downarrow\uparrow, -\vec{e}_x\rangle$	$-if_q e^{\frac{ik_x}{2}}$	0	$F_q^r e^{\frac{ik_x}{2}} + F_{\bar{q}}^r e^{-\frac{ik_x}{2}}$	$if_{\bar{q}} e^{-\frac{ik_x}{2}}$
$ \psi_3, \downarrow\downarrow, -\vec{e}_x\rangle$	0	$-if_{\bar{q}} e^{\frac{ik_x}{2}}$	$-if_q e^{-\frac{ik_x}{2}}$	$F_q^r e^{\frac{ik_x}{2}} + F_{\bar{q}}^r e^{-\frac{ik_x}{2}}$

REFERENCES

- [1] M. Burkardt, *Advances Nucl. Phys.* **23**,1 (1996).
- [2] K. Wilson et al., *Phys. Rev. D***49**, 6720 (1994).
- [3] W.A. Bardeen, R.B. Pearson, and E. Rabinovici, *Phys. Rev. D***21**, 1037 (1980)
- [4] M. Burkardt, invited talk given at “11th International Light-Cone School and Workshop”, Eds. C. Ji and D.-P. Min, hep-th/9908195.
- [5] P. Griffin, *Proc. to Theory of Hadrons and Light-Front QCD*, Ed. S. Glazek, World Scientific, Singapore, 1994.
- [6] M. Burkardt and B. Klindworth, *Phys. Rev. D***55**, 1001 (1997)
- [7] S. Dalley and B. vande Sande, *Phys. Rev. D***59**, (1999); *Phys. Rev. Lett.***82**, 1088 (1999); *Nucl. Phys. B (Proc. Suppl.)***83**, 116 (2000); *Phys. Rev. D***62**,(2000)
- [8] M. Burkardt and H. El-Khozondar, *Phys. Rev. D***60**, (1999)
- [9] S. Dalley, *Nucl. Phys. B (Proc. Suppl.)***90**, 227 (2000)
- [10] S.K. Seal and M. Burkardt, *Nucl. Phys. B (Proc. Suppl.)* 90, 233(2000)
- [11] S. Dalley, hep-ph/0101318.
- [12] M. Burkardt and S. Seal, hep-ph/0101338.
- [13] M. Burkardt, *Phys. Rev. D* **57**, 1136 (1998).
- [14] M. Burkardt and S. Seal, Invited talk at 5th International Workshop on Particle Physics Phenomenology, Chi-Pen, Taitung, Taiwan, 8-11 Nov 2000; hep-ph/0101338.
- [15] S. Dalley, private communications.

FIGURES

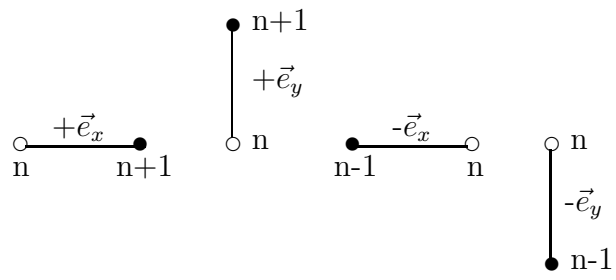


FIG. 1. Four possible orientations of the 3-particle states.

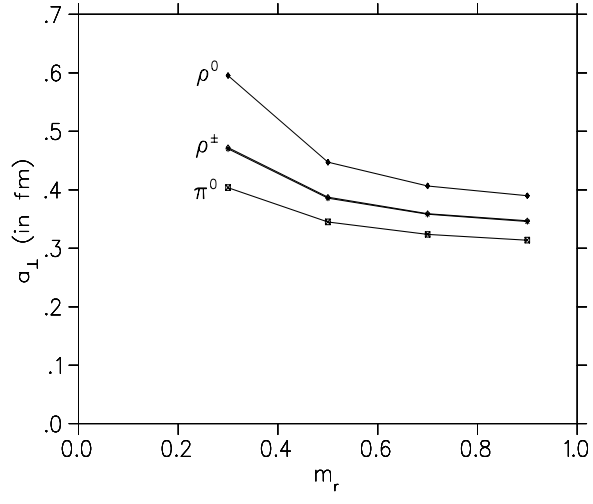


FIG. 2. Dependence of a_{\perp} on the non-spin flip coupling.

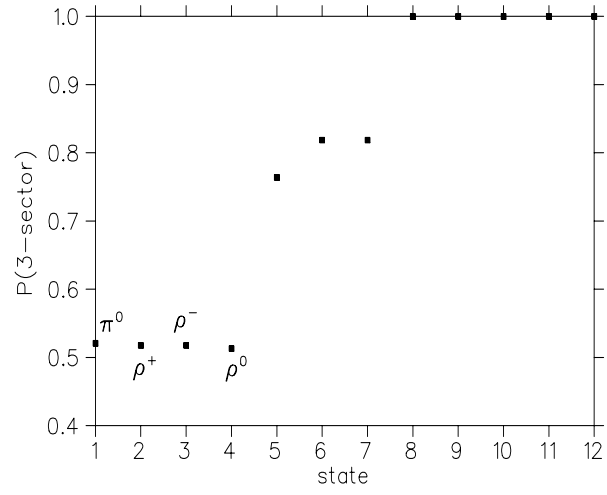


FIG. 3. Probability of states to be in the 3-particle sector.

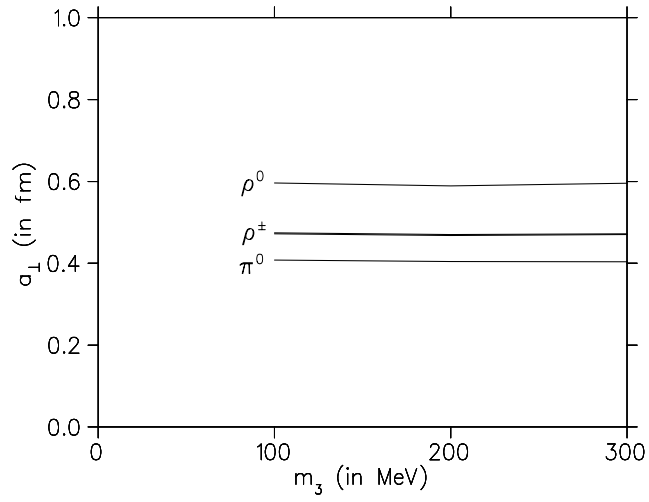


FIG. 4. Dependence of the \perp lattice spacings on the masses in the 3-particle Fock component (other parameters are adjusted correspondingly to keep the physical π and ρ masses fixed).

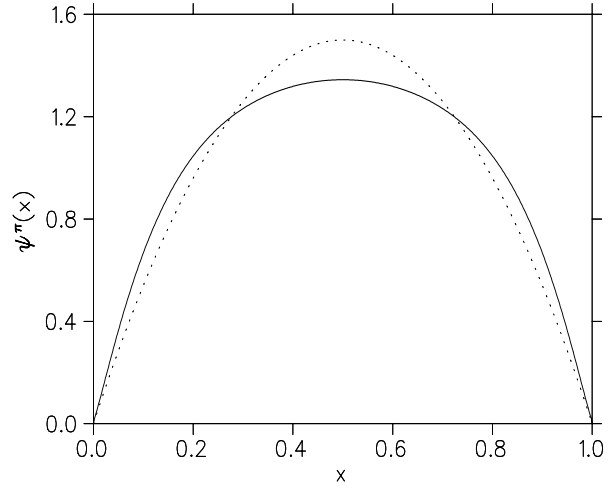


FIG. 5. Light-cone momentum distribution amplitude for the π obtained on the \perp lattice. The dashed line is the asymptotic shape.

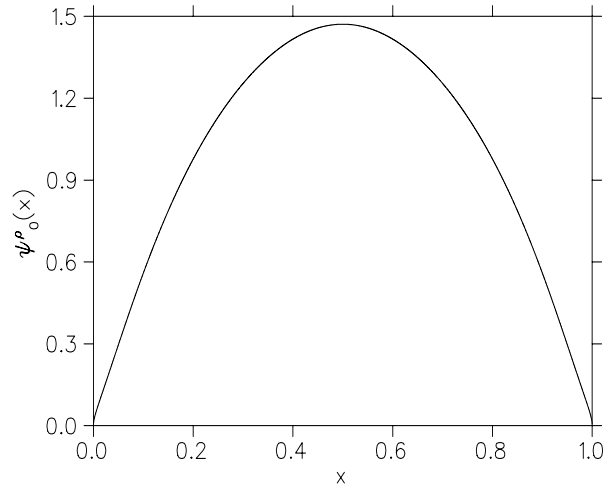


FIG. 6. Light cone distribution amplitude for ρ^0 obtained on the \perp lattice.

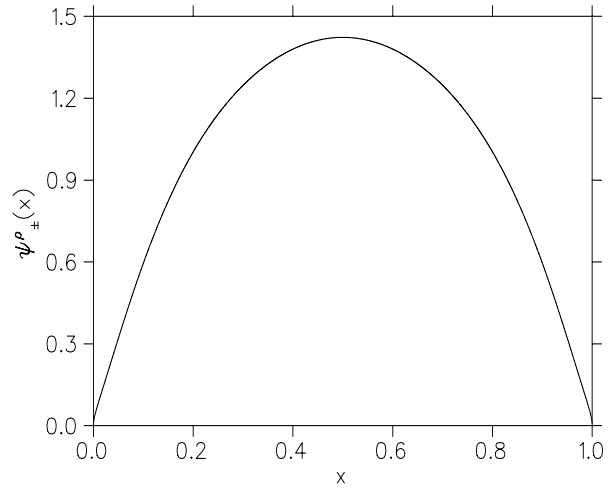


FIG. 7. Light cone distribution amplitude for ρ^\pm obtained on the \perp lattice.

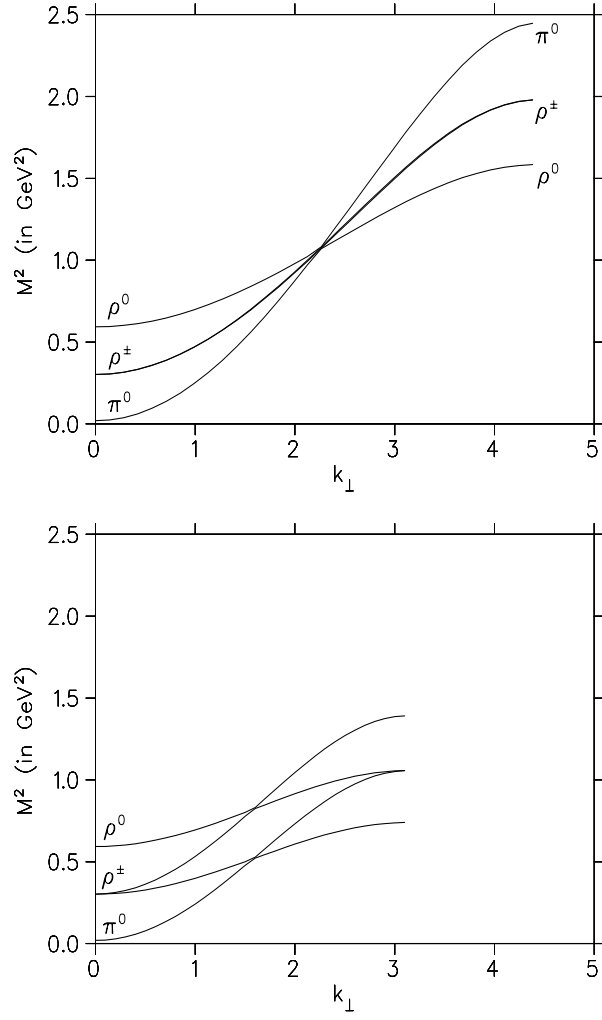


FIG. 8. The diagonal(top) and parallel(bottom) dispersion relations for the π and ρ mesons.

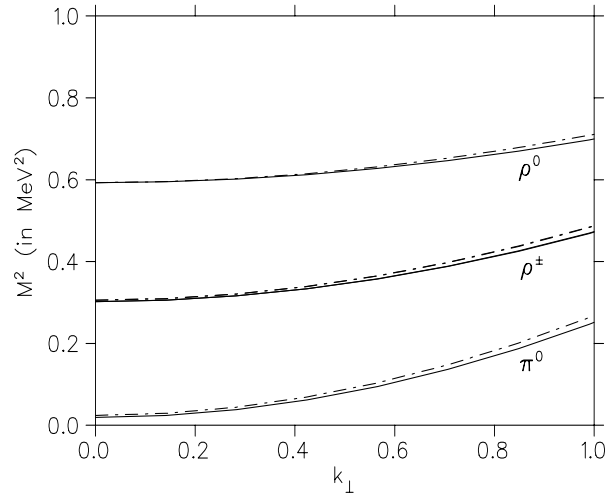


FIG. 9. ϵ independence of dispersion relations. The dashed line is for $\epsilon = 0.05$ and the continuous line is for $\epsilon=0.1$.

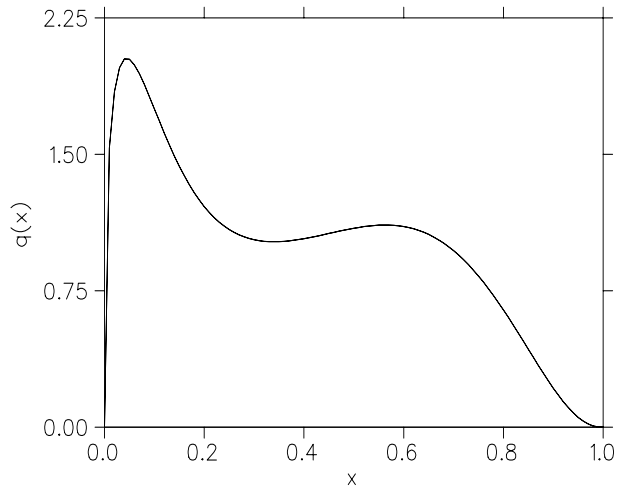


FIG. 10. Pion parton distribution function.

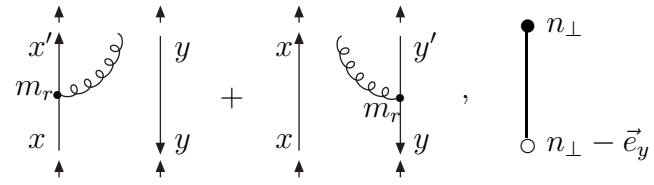


FIG. 11. Spin non-flip hopping.

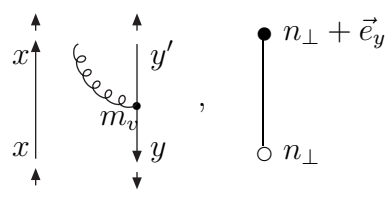


FIG. 12. Spin flip hopping.